NOx Storage and Reduction with Propylene on Pt/BaO/Alumina

Rachel L. Muncrief, Karen S. Kabin, and Michael P. Harold
Dept. of Chemical Engineering, The University of Houston, Houston, TX 77204

DOI 10.1002/aic.10208
Published online in Wiley InterScience (www.interscience.wiley.com).

An experimental study was carried out of periodically operated NOx ($NO + NO_2$) storage and reduction on a model $Pt/BaO/Al_2O_3$ catalyst powder. The effect of the reductant (propylene) injection policy on time-averaged NOx conversion was evaluated in terms of feed composition and temperature, reductant pulse duration, and overall cycle time. Conditions giving time-averaged NOx conversions exceeding 90% were identified. The reductant-to-oxidant ratio during the injection and the total cycle time are both found to be critical factors to achieve high conversion. The time-averaged conversion is bounded above and below by the steady-state conversions obtained with feeds having the same compositions as that during the rich and lean part of the cycle, respectively. For a fixed supply of propylene, short pulses of high concentration are much more effective than longer pulses of reduced concentration. The NOx conversion achieves a maximum value at an intermediate overall cycle time when the propylene pulse of fixed duty fraction is net reducing. High conversions are sustained over a wide temperature window (200–400°C). A simple storage–reduction cycle is proposed that elucidates the main findings in the study. The key factor for high NOx conversion is the temporal production of oxygen-deficient conditions coupled with high catalyst temperatures, both resulting from the intermittent catalytic oxidation of propylene.
AIChE J, 50: 2526–2540, 2004
Keywords: NOx, diesel, emissions, catalysis, reaction engineering, NOx trap, NOx storage and reduction

Introduction

With fossil fuels serving as the primary energy source for the foreseeable future, it is critical that the fuel efficiency of the vehicular fleet be increased at minimal cost to the economy. Diesel-powered vehicles offer improved fuel efficiency compared to their spark-ignited, gasoline-powered counterparts (Clerc, 1996; Diesel Technology Forum, 2001; Farrauto and Voss, 1996; Frost and Smedler, 1995; Herzog, 1997; Lox et al., 1990). However, diesel engine exhaust has many adverse environmental effects because of the emission of nitrogen oxides (NOx), particulate matter (PM), and SO_2. There is a pressing need to develop diesel emission control technology to take full advantage of the fuel efficiency and durability of diesel vehicles. Emission standards for heavy-duty diesel vehicles require more than a 90% reduction in total particulate matter and NOx (TCEQ, 2003). These standards place new demands on improved engine performance and catalytic converter technology.

The lean burn conditions of diesel combustion that yield higher combustion temperature and improved efficiency produce an exhaust having an excess of oxygen. This net-oxidizing atmosphere enables the straightforward oxidation of hydrocarbons and CO with conventional precious metal catalysts, although it undermines conventional approaches to chemically reduce NOx. Considerable research and development has been carried out in the last 5–10 years on diesel/lean-burn exhaust abatement of NOx. The different catalytic approaches are summarized below.

Correspondence concerning this article should be addressed to M. P. Harold at mharold@uh.edu.

Selective catalytic reduction (SCR), involving ammonia (as the reductant) and $V_2O_5/WO_3/TiO_2$ catalyst, follows from its successful deployment in stationary source emission NOx abatement. However, this application requires the use of onboard anhydrous ammonia or aqueous urea injection, which poses safety and reliability issues (Farrauto and Voss, 1996; Shelef, 1995; van Kooten et al., 1997). The direct decomposition of NO requires at least a factor of 10 increase in best reported activities (with Cu/ZSM-5) and improvement in stability (Armor and Li, 1995). Similar activity and stability improvements are needed for (steady-state) selective catalytic reduction with hydrocarbons under lean conditions (Armor and Li, 1995). Although recent progress has been made with zeolite-based catalysts (Traa et al., 1999), steady-state NOx conversions are still too low and the operating window is too narrow.

NOx storage and reduction (NSR) or "NOx trap" technology is a promising NOx-abatement approach for mobile diesel sources. First proposed by Toyota in the mid-1990s, NSR involves the oxidative adsorption of NOx on an alkali earth oxide (such as barium oxide), forming a surface nitrate (Miyoshi et al., 1995; Takahashi et al., 1996). The nitrate is then chemically reduced by periodic "rich" operation of the lean burn engine, which increases the level of hydrocarbons in the exhaust to promote the reduction of NOx. Recent research efforts have focused on broadening the possible uses of the NSR concept (Bogner et al., 1995; Czamecki et al., 2000; Feeley et al., 1997; Fridell et al., 1997; Han et al., 2001; Ladommatos et al., 2000; MECA, 1999). Engelhard Corp. (Iselin, NJ) proposed an NSR system of two sequential reactors for use in diesel vehicles (Feeley et al., 1997). Others have proposed recycling the adsorbed NOx back to the engine where it is decomposed (Ladommatos et al., 2000); and some have elucidated the performance of selected catalysts (such as Rh/β-zeolite) during rich–lean cycling (Han et al., 2001). Others have found ways of improving the NOx trap capabilities of these catalysts (Fridell et al., 1999; Lietti et al., 2001; Salasc et al., 2002), such as innovative preparation techniques, and selective additives. Matsumoto (2000) discussed adding TiO_2 and using a hexagonal monolith substrate to reduce the impact of sulfur poisoning. Narula et al. (2001) found that sol–gel-processed NOx traps have increased NOx trapping efficiency and respond better to high-temperature regeneration than catalysts prepared through standard impregnation techniques. Theis et al. (2003) found that the addition of rhodium reduces the amount of NOx released during the addition of the reductant.

Several studies have appeared that discuss possible mechanisms. Early studies by Bögner et al. (1995) used simulated exhaust gas and engine exhaust to determine the performances of various NSR catalysts. They concluded that the catalyst stores NO_x as a surface metal nitrate. They also determined that the catalyst was fully regenerable under rich conditions. Rather high time-averaged NOx conversion (94%) was obtained using 30-s lean and 30-s rich cycle times. Amiridis and coworkers used *in situ* FTIR to study NO adsorption on Pt/Al_2O_3 catalysts and found that at 250°C NO will adsorb on the Al_2O_3 as well as the Pt, but that the Pt adsorbed species are not stable in the presence of O_2 (Captain and Amiridis, 1999). Takahashi et al. (1996) used FTIR to conclude that NO is oxidized to NO_2 on the Pt sites and then stored as a surface nitrate on adjacent Ba sites. During the rich phase, the NOx is released from the Ba site and reduced on the adjacent Pt site. They also experimentally determined that the NOx conversion is highly dependent on the stoichiometric ratio, but independent of the actual reducing agent. Fridell et al. (1997) proposed a similar reaction scheme in which the reaction step leading to stored NOx involved NO_2 and atomic oxygen. Huang et al. (2001) compared adsorption rates of NO and NO_2 using various noble metal and CaO catalysts. They also concluded that the NO_2 adsorption rate is much higher than that of NO, and the noble metal catalyst is advantageous in converting NO to NO_2. Olsson et al. (2002) were able to successfully model NOx storage on $Pt/BaO/Al_2O_3$ with reduction by propene. The model was able to predict the typical NOx breakthrough seen during the lean storage phase as well as the sharp NOx breakthrough peak seen when switching from lean to rich mixtures.

Other studies have focused on the effects of key parameters of the NOx storage and conversion. Fridell et al. (1999) showed that the NOx storage has a strong dependency on temperature, with a maximum storage observed around 380°C. They also confirmed the findings of Takahashi et al. (1996) that a correlation exists between higher oxygen concentrations and higher NOx storage capacity. Han et al. (2001) studied the effects of a wider range of stoichiometric ratios during the rich period as well as variations on the durations of the rich and lean periods. They concluded that to optimize the cycle, the reductant pulse must be rich enough to fully regenerate the adsorption capacity of the catalyst and fast enough to minimize inhibition by CO and C_3H_6 admolecules. Lietti et al. (2001) discussed the effects of temperature on NOx storage and the inhibiting effect of CO_2 on NOx storage and reduction. Nova et al. (2002) asserted that there are multiple adsorption sites involved in the adsorption of NOx and that the adsorption occurs first on the BaO sites and then on $BaCO_3$ sites, which is a slower process. They also found that at lower temperatures the selectivity of nitrate to N_2 is reduced because of the generation of NO from nonselective Pt–O species. Eigneberger and coworkers proposed a shrinking core mechanism for NOx storage (Tuttlies et al., 2003). Their postulate is that an outer shell of barium nitrate forms on the barium carbonate particles, contained within the pore of the supported catalyst, during the NOx storage process using CO as the reductant. They note that $BaCO_3$ has approximately half the specific volume of $Ba(NO_3)_2$, so as storage occurs the particles expand, and NO diffusion through the nitrate layer limits the storage rate. Upon the introduction of the CO reductant, the formation of a regenerated shell of carbonate forms on the outer layer of the barium particle, and the process repeats itself.

Although advances have been made with NOx storage and reduction, there are obstacles toward its widespread deployment in lean-burn diesel vehicles.

Fuel consumption

NSR used in lean-burn, spark-ignited vehicles requires intermittent rich engine operation to produce an exhaust for NOx release and reduction. Diesel engines require direct fuel injection in the exhaust to release NOx from the adsorbent and to reduce the surface nitrate to molecular nitrogen. A greater than 3% reduction in fuel economy resulting from either operating scheme would be unacceptable (MECA, 1999). Determining

the requisite fuel consumption to achieve a high NOx conversion is essential in assessing the viability of NSR.

Reductant type and injection policy

Lean-burn and diesel exhaust contains up to 1000 ppm of volatile NOx reductants such as CO and hydrocarbons. The specific composition of the hydrocarbon fraction depends on the engine operation, but generally will be a mixture of lower molecular weight olefins and alkanes. Most studies of NSR have used H_2, CO, or low molecular weight alkanes or olefins (often propylene) as the reductant(s). This may be reasonable during rich operation of a lean-burn engine, although direct injection of diesel fuel into the exhaust system introduces a more complex mixture of hydrocarbons. Moreover, because injection is deliberate, the injection policy becomes a key operating variable that should be optimized. The literature suggests that the reductant type can have an important effect on the converter performance. Burch and Millington (1995) reported differences in the effectiveness of several reductants on the lean NOx conversion over Pt-supported catalysts. Few studies have appeared that have evaluated the reducing efficacy or the injection policy of simple reductants, diesel fuel, or common diesel components. A recent study of Los Alamos researchers (Ott et al., 2002) shows that the autothermal reforming of diesel fuel on a precious metal catalyst yields a mixture of CO, H_2, and low molecular weight olefins. These species are effective reductants of NOx.

Converter dynamics and control

NSR is a transient process with deliberate cycling of lean (engine exhaust) and rich (fuel added) mixtures. Moreover, the exhaust composition and flow rate vary according to the engine operation. Clearly, robust operating protocols and control algorithms must be developed for the NSR converter, which ensure pollution abatement under these intrinsically unsteady conditions.

Catalyst durability and sulfur tolerance

The NSR catalytic adsorbent must maintain good performance over repeated cycling and exposure to components such as sulfur dioxide (SO_2), H_2O, and CO_2 at elevated temperatures. Model systems (such as $Pt/BaO/Al_2O_3$) have demonstrated good performance, but reduced effectiveness in the presence of steam and CO_2, and particularly poor sulfur tolerance (Amberntsson et al., 2003; Lee and Rhee, 2002; Rodrigues et al., 2001). Sulfur poisoning is the primary obstacle in the implementation of NOx adsorber technology (MECA, 1999). Sulfur levels found in conventional diesel fuel grades (500–5000 ppm S) lead to high levels of exhaust SO_2. The SO_2 reacts with the rare earth promoter, leading to reduced adsorptive capacity and catalytic activity (Borup et al., 2003). Desulfurization of the NOx trap catalyst is needed to restore reactivity. This high-temperature reactivation can lead to sintering and reduced NOx trapping. A more sulfur-tolerant NSR catalyst is needed to reduce the detrimental impact on catalyst life.

In the current study, we focus on the reductant injection policy and reactor dynamics performance issues. Performance of a model $Pt/BaO/\gamma\text{-}Al_2O_3$ catalyst powder is investigated using propylene as the reductant, with specific attention paid to the effect of reductant injection policy on time-averaged NOx conversion, and the effect of feed composition under steady state and periodic operation. We identify the operating conditions that give a high time-averaged NOx conversion. The results of this study provide insight into the interacting catalytic and transport processes that occur during the complete NSR cycle.

Experimental

Catalyst preparation

For this study a typical NOx storage catalyst (powder) was used, $Pt/BaO/Al_2O_3$ (1/20/100 w/w/w), prepared using standard techniques. The γ-alumina support (97.7%, Strem Chemicals, Newburyport, MA) was first calcined in air for 1 h at 550°C. A small amount of the calcined support was immersed in a 0.1 molar solution of barium nitrate [99% $Ba(NO_3)_2$, Johnson Matthey Plc, London, U.K.]. The mixture was stirred while being heated at 80°C for 2 h, and was then dried in an oven overnight at 110°C. The barium–alumina sample was then calcined in air for 1 h at 550°C to remove any residual precursor and to oxidize the barium. The sample was then impregnated with platinum, by incipient wetness, using tetraammineplatinum (II) hydroxide solution (9.18 wt. % Pt; Johnson Matthey) as the precursor. The solution was diluted to make a 0.5 wt. % platinum solution. Diluted platinum solution was added dropwise to the BaO/Al_2O_3 powder. The mixture was then dried in an oven overnight at 110°C. The final sample was calcined in air for 1 h at 550°C and then reduced in flowing hydrogen at 500°C for 1 h. Actual platinum content is 0.5 ± 0.05 wt %, and actual barium content is 12.32 ± 1.2 wt. % as measured by ICP-OES (Galbraith Laboratories, Knoxville, TN).

The catalyst has a surface area of 140 m^2/g, an average particle size of 55 μm, and a platinum dispersion of 47%. The platinum dispersion was measured by hydrogen-pulse chemisorption. Known volumes of hydrogen were pulsed over the catalyst at room temperature and the hydrogen breakthrough was measured by a gas chromatograph (model 6890N; Agilent Technologies, Palo Alto, CA) with a TCD detector and a molecular sieve (Type 5a, 80/100 mesh) packed column. The catalyst surface area was measured with a BET (model SA3100; Beckman Coulter, Fullerton, CA) using N_2 adsorption.

Steady-state studies

The NOx storage catalyst described above was studied in a variety of steady-state and cycling experiments. The experimental setup used is shown in Figure 1. The gas-delivery system consisted of a series of gases used to simulate a lean exhaust. In the current study the feed gas contained a mixture of NO, C_3H_6, and O_2 in a nitrogen carrier. A small amount of the NO in the feed will convert to NO_2 when O_2 is present; in a feed of 500 ppm NO and 5% O_2, for instance, 2% of the NO will convert to NO_2 at 110°C (the temperature of our gas lines). This conversion increases linearly with O_2 concentration. The flow rates of the gases were controlled with precision mass flow controllers (MKS Instruments, Wilmington, MA) programmed using LABTECH software (Andover, MA). The total

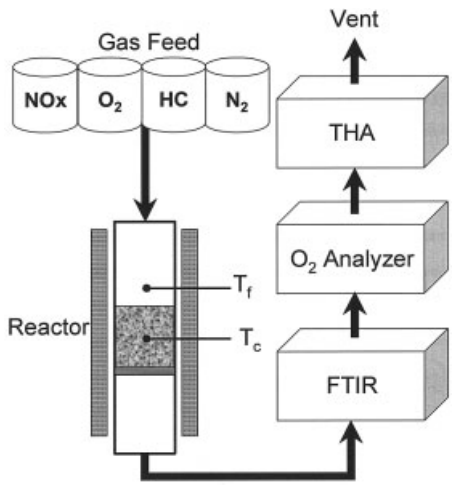

Figure 1. Gas feed, reactor, and analysis setup.

gas flow rate was kept constant at 200 cm^3/min; individual concentrations of NO, C_3H_6, and O_2 were varied over selected ranges specified below. The gases were mixed in an in-line static mixer, and then sent through a tubular quartz packed-bed reactor positioned inside a tube furnace. The packed bed of catalyst was placed on a medium porosity quartz frit. The reactor contained 207 mg of catalyst (0.28 cm^3 volume) without dilution. For the stated flow rate the gas space velocity (GHSV) was 42,000 h^{-1} (at standard conditions 0°C, 101.3 kPa). The reactor temperature was monitored with two K-type thermocouples, one positioned just upstream of the catalyst (~ 3 cm) and the other positioned in the center of the catalyst bed. Hereafter we refer to these as the feed (T_f) and catalyst (T_c) temperature, respectively. These temperatures were continually monitored during reaction studies.

The outlet gases flowed through heated lines (110°C) to a gas phase analysis system composed of an FTIR spectrometer, O_2 analyzer, and THC analyzer. The FTIR (Thermo-Nicolet Nexus 470; Nicolet Analytical Instruments, Madison, WI) was equipped with a specialty ultralow-volume (25 cm^3) gas cell (Mini Linear Flow Cell; Axiom Diagnostics, Cork, Ireland). At the flow rate of 200 cm^3/min, the gas residence time was about 7.5 s. The setup allows for the on-line analysis of products with a scan rate of two spectra/s. The species detected in this study were NO, NO_2, N_2O, CO, CO_2, H_2O, and C_3H_6. The FTIR was calibrated by feeding known concentrations of each species and correlating the concentration with the intensity of the main bands from the IR spectra of each component. Manufacturer-provided software (Omnic Series and Omnic QuantPad, Thermo Electron Corp., Woburn, MA) enabled a quantitative analysis of the products in real time. We routinely reviewed the product spectra for IR bands of other species during the experiments, such as NH_3, but no detectable amounts of any other reaction products were found. After passing through the FTIR, the gases flowed through a gas dryer and then to a thermogravimetric O_2 analyzer (Oxymat 61; Siemens, Erlangen, Germany). Finally, the product gases flowed to a total hydrocarbon analyzer (THA) with a flame ionization detector (FID; Model 8800, Baseline-Mocon, Lyons, CO) where a total hydrocarbon analysis was accomplished (on a methane basis). To synchronize the outputs from our multiple analyzers, tracer studies were carried out at 200 cm^3/min to determine the time delays between all points in the experimental system.

Two types of steady-state experiments were carried out to examine NOx storage and conversion efficiency as a function of several operating parameters. The feed composition was characterized by the stoichiometric number (S_N), defined as the ratio (molar) of the oxidizing to the reducing components. For the purpose of this study S_N is defined as

$$S_N = \frac{2[O_2] + [NO]}{9[C_3H_6]} \tag{1}$$

where [·] denotes the molar concentration.

Measurement of the storage properties of the catalyst was achieved by monitoring the NOx uptake as a function of the feed temperature and the NO partial pressure. In a typical storage experiment we fed a mixture of NO and O_2 (in N_2) over the catalyst until the NOx effluent concentration equaled the feed value (within 1%). Before storage studies, the catalyst was purged with 1000 ppm C_3H_6 for 25 min at the adsorption temperature to convert the barium to carbonate form sites (as there would be under reaction conditions). Total NOx uptake was determined by desorbing NOx from the catalyst by a temperature ramp to 550°C, with the amount desorbed determined by FTIR measurement. To obtain steady-state conversion data, the desired feed temperature was set, then prescribed amounts of NO, O_2, and C_3H_6 were fed to the reactor until the NOx outlet reached steady state. Conversion was calculated by dividing the amount of NOx reacted by the amount of NOx fed to the system (where the amount of NOx reacted is the amount of NOx in minus the amount of NOx out). Selectivity to N_2 was determined by the amount of NOx reduced to N_2 ratioed to the total NOx consumed. The NOx reduced to N_2 was computed as the difference between the total NOx reacted and the NOx converted to N_2O: NOx to N_2 = NOx reacted − $2N_2O$ formed.

Lean-rich cycling studies

The gas flow system for the lean/rich cycling experiments was the same as that of the steady-state experiments (Figure 2). The lean gas feed mixture composition was kept constant at 500 ppm NO, 5% O_2, and 1000 ppm C_3H_6 in nitrogen. During the rich period oxygen flow was maintained to simulate a diesel engine system in which reductant (such as fuel or reformed fuel) is injected into the exhaust. Propylene was chosen as the reductant for these studies primarily because it has a relatively low light-off temperature and clean burn characteristics, and it is a popular reductant in other SCR and NSR studies, enabling a basis for comparison. It was added at a prescribed flow rate and feed duration (or duty cycle). Pulsing was accomplished with the computer-operated mass flow controllers. Some spreading of the square pulses occurred as a result of dispersion. We return to this point in the interpretation of some of the data. The independent variables included feed temperature, total cycle time, reductant feed concentration, and reductant duty cycle (percentage of total cycle with reductant fed). We investigated the individual effects of these variables on the time-averaged conversion of NOx (that is, NO and NO_2 conversion to all other N-containing products), selectivity of NOx to N_2, and breakthrough of C_3H_6 and CO. In a typical exper-

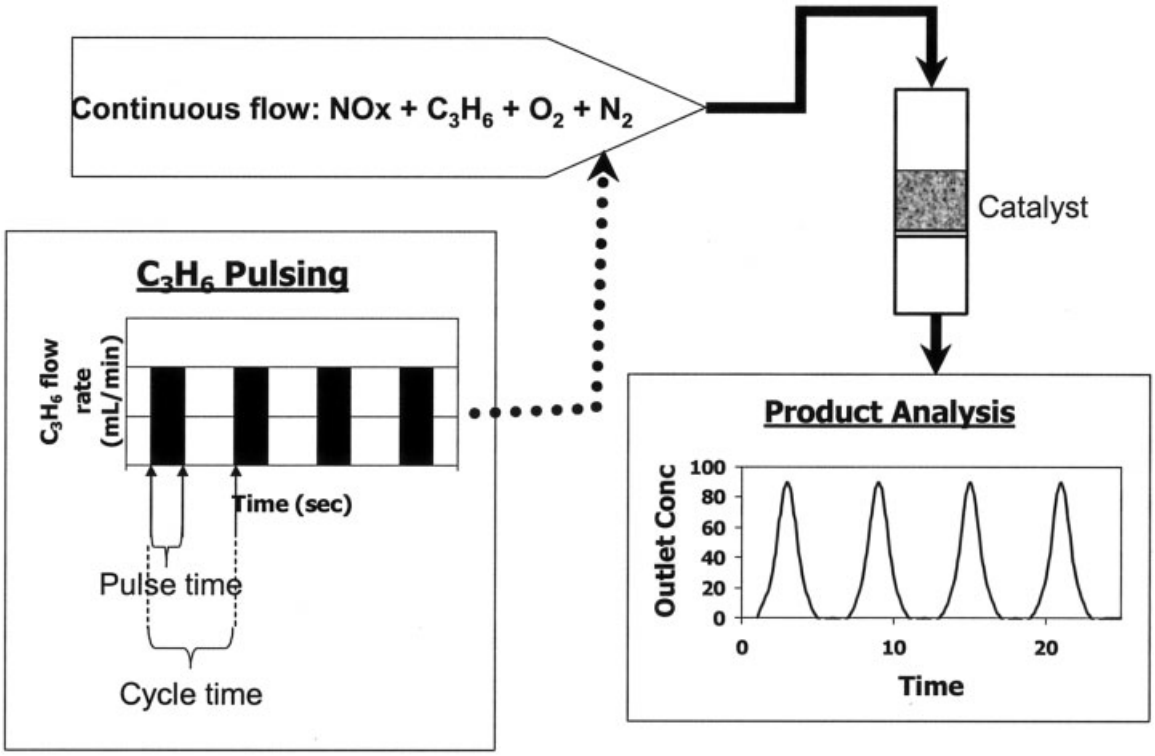

Figure 2. Gas flow system for the lean/rich cycling experiments.

iment, time-averaged quantities were obtained over 10 cycles. We periodically checked the catalytic activity by repeating the experimental conditions of steady-state lean NOx conversion at 250°C. If there was any loss in activity the catalyst was regenerated by recalcining in oxygen for 120 min. This procedure was needed in the present study only when carbonaceous species were formed on the catalyst, caused by long injections of a hydrocarbon-rich feed.

Results

NOx storage and capacity

Figure 3 shows NOx breakthrough as a function of time when NO (500 ppm) and O_2 (5%) were fed at a feed temperature of 350°C over catalyst initially reduced with hydrogen at 500°C. There are two stages. The first stage is a short, initial period during which there is no NOx breakthrough. This is followed by a second stage during which NOx breakthrough occurs and the effluent NOx concentration increases, but with a declining slope. The NOx concentration asymptotically approaches the feed concentration (500 ppm) at long times, at which point the net rate of NOx accumulation on the catalyst is zero within the detection limits of the FTIR. Storage of NOx occurs during both stages until complete breakthrough occurs. For the case shown, the first stage had a duration of 42 s. About 47 min were needed to reach 495 ppm (that is, within 1% of the feed value).

The "long-time" NOx storage capacity was measured as a function of the temperature and NOx feed concentration. In this set of experiments we waited for the NOx breakthrough to reach steady state, purged the system with N_2 (until there was zero NOx breakthrough), then heated the catalyst until all NOx desorbed, the quantity of which was quantified by FTIR. The storage isotherms at three different temperatures are shown in Figure 4. The total amount of NOx stored increases with NOx concentration. For a fixed NOx concentration, the "long-time" NOx capacity decreases with increasing temperature.

The dynamic NOx storage capacity is defined as the amount of NOx stored during the first stage of complete NOx trapping. This storage value is an important quantity because it represents the amount of NOx trapped before the introduction of reductant, which, as we describe below, may occur with a period on the same order as the NOx breakthrough time. We measured the dynamic NOx storage by exposing an initially

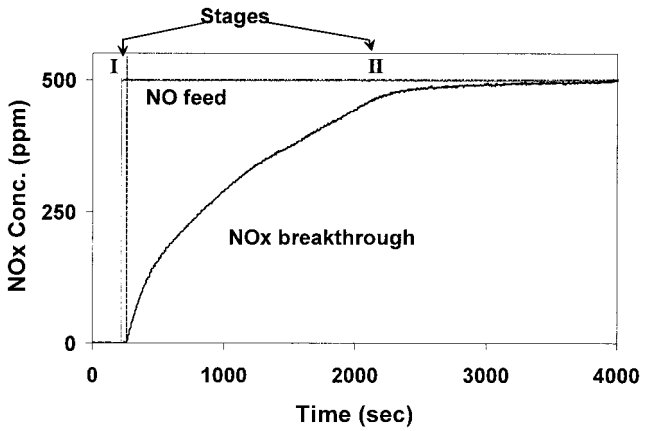

Figure 3. Stages of NOx breakthrough over a Pt/BaO/Al_2O_3 catalyst at 350°C with a feed of 500 ppm NO and 5% O_2.

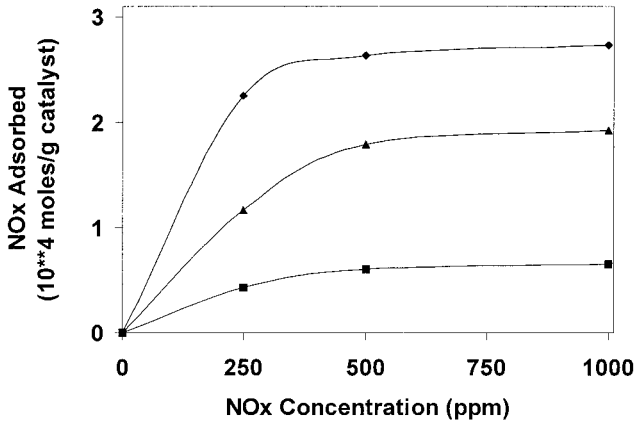

Figure 4. NOx storage isotherms for 300 (◆), 350 (▲), and 400°C (■), for a flow of varying concentrations of NO and 5% O_2.

These data are "long-time" storage when the effluent NOx was within 1% of the feed concentration.

reduced catalyst to a flow of 500 ppm NO and 5% O_2 for a prescribed period of time. The total time lapse until detectable NOx breakthrough occurred was used to determine the moles of NOx stored per gram of catalyst. The dependency of dynamic storage capacity on feed temperature is shown in Figure 5. The storage exhibits a maximum at about 350°C. For comparison, the long-time NOx storage is also shown in the figure.

Steady-state NOx reduction

The steady state performance of the catalyst was examined over a range of feed compositions spanning rich to lean. Figure 6 shows the NOx conversion as a function of the stoichiometric number for a feed temperature of 250°C, space velocity of 42,000 h^{-1}, and feed gas containing 500 ppm NO and 1.5% C_3H_6. The feed oxygen concentration was varied to span a wide range of stoichiometric number values (S_N = 0.1–10). The NOx conversion is less than 20% with lean mixtures and approaches 100% for rich mixtures. A sharp conversion change occurs at the stoichiometric number of approximately unity, the transition between rich and lean. The catalyst temperature

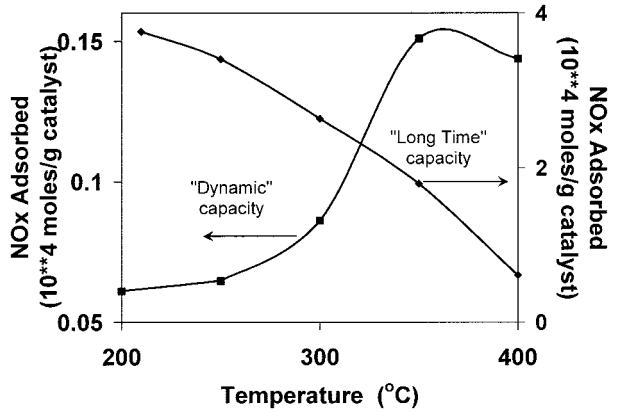

Figure 5. Dynamic (■) and "long-time" (◆) storage of $Pt/BaO/Al_2O_3$ catalyst vs. temperature for a flow of 500 ppm NO and 5% O_2.

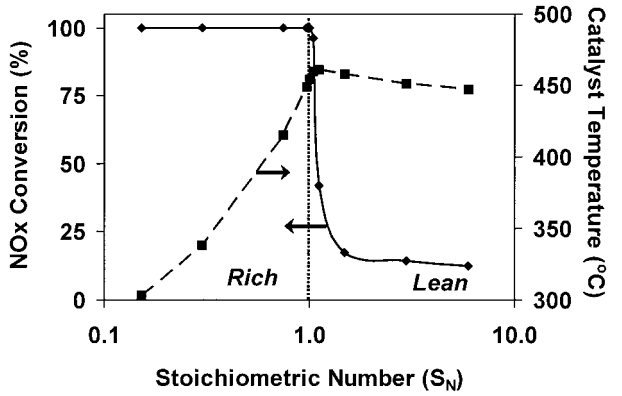

Figure 6. Steady-state NOx conversion (◆) and catalyst temperature (■) vs. S_N for a flow composition of 500 ppm NO, 1.5% C_3H_6, and varying O_2.

exhibits a maximum value (460°C) for the S_N = 1 feed mixture (that is, feed gas contains 1.5% C_3H_6 and 6.75% O_2).

The effect of feed temperature on the NOx conversion is shown in Figure 7a for both lean (S_N = 11.2; 0.1% C_3H_6 5% O_2) and rich (S_N = 0.53; 2.1% C_3H_6 5% O_2) feed gases. Light-off occurred for both feeds at about 200°C, leading to a sharp increase in the NOx conversion (and propylene conver-

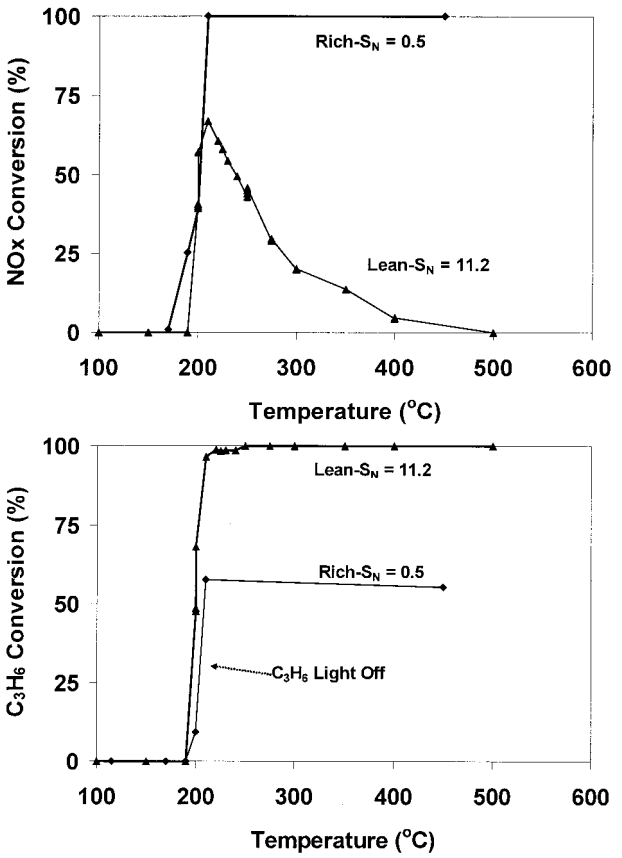

Figure 7. (a) Steady-state NOx conversion vs. feed temperature for a rich feed of S_N = 0.5 (◆) and lean feed of S_N = 11.1 (▲); (b) C_3H_6 conversion vs. temperature for the same feeds as in (a).

sion, shown in Figure 7b). The lean feed exhibited a peak conversion (~ 45%) between 200 and 250°C, whereas the rich feed gave a high conversion for the entire range of temperatures.

NOx storage and reduction cycling

In the next phase of our experimentation we cycled between lean and rich conditions by injecting varying amounts of propylene (reductant) into the feed. Figure 8 shows 10 periods of a typical cycling experiment. A more detailed view of two propylene injections is shown in Figure 9. Shown are the catalyst temperature and effluent NOx (and NO_2), N_2O, C_3H_6, CO_2H_2O, CO, and O_2 concentrations. In this experiment the feed temperature was 330°C, the cycle time was 70 s, and the propylene pulse had a duration of 12 s. Approximately 0.60 standard cm^3 propylene (2.7e-5 mol) was injected during each pulse (S_N = 0.7 during pulse). The injection of propylene caused a noted increase in the catalyst temperature and CO_2 and water concentration, and a decrease in the oxygen concentration, indicating exothermic catalytic oxidation. During the oxidation a short excursion in effluent NOx ($NO + NO_2$) was observed, followed by a sharp decrease to near zero. The NOx breakthrough commenced shortly thereafter, gradually increasing during the lean period until the next propylene pulse was admitted. Small increases in CO and N_2O concentrations were detected during the propylene pulse.

The effect of the rich pulse concentration on the NOx conversion is shown in Figure 10a. In this experiment we fixed the total cycle time at 70 s and the percentage rich duty cycle at 14% (10-s duration). The 350°C lean feed constituted a mixture of 500 ppm NO, 5% O_2, and 1000 ppm C_3H_6. The propylene feed rate was adjusted to span a wide range of "rich feed" compositions (S_N = 0.1–10). Without pulsing, the steady-state NOx conversion was about 18%. As the propylene concentration was increased and the S_N approached unity, the conversion very gradually increased. A sharp increase in conversion occurred when the propylene concentration in the pulse exceeded 2.1% (S_N = 0.53). For S_N values less than 0.53, the time-averaged conversion was sustained at about 90%. Also shown in Figure 10a is the dependency of the cycle peak temperature of the catalyst. The results show a large increase in the peak temperature as the propylene concentration in the pulse increased. Figure 10b shows the dependency of the conversion on the time-averaged feed composition (S_N). The results reveal a high NOx conversion (>90%) even when the cycle-averaged feed concentration was lean (S_N = 1–3). For a detailed view of the difference in NOx conversion between S_N = 0.7 and S_N = 0.53, Figure 11a shows NOx outlet vs. time for the pulsing experiment in Figure 10, and Figure 11b shows catalyst temperature vs. time for these two experiments.

The dependency of the time-averaged NOx conversion on rich pulse composition was determined for several feed temperatures (Figure 12). The conversion in the rich pulse regime was insensitive to temperature but there was a large variation in the lean pulse regime. In the rich regime the conversion exceeded 90% for a feed temperature as low as 210°C. (Below 200°C the propylene oxidation did not light off and conversions for NOx and propylene were very low.) In the lean regime the conversion increased with decreasing feed temperature.

To isolate the effect of pulsing from the pulse composition, we carried out a set of experiments in which the total propylene pulsed was fixed, but the duty cycle was varied. Figure 13 shows the results for the same feed as before (70-s cycle; 350°C feed; 500 ppm NO; 5% O_2) with a fixed pulse volume of propylene of 0.67 standard cm^3 (3e-5 mol). The hydrocarbon pulses varied from short, very rich pulses, to long, less-concentrated pulses. The results in Figure 13a show that short, rich pulses are much more effective than longer, leaner pulses. Between 28 and 14% duty cycle rich the time-averaged NOx conversion increases from below 30% to over 90%. Measurement of effluent CO and propylene effluent concentrations revealed a sharp increase in the same regime. Figure 13b shows the dependency of the rich pulse composition (S_N) as a function of the duty cycle. Consistent with earlier findings, the sharp increase in conversion corresponds to the transition from a lean to rich pulse.

Figure 14a shows the effect of the feed temperature on the NOx conversion and NOx to N_2 selectivity. The conversion increases sharply at 200°C. A high time average NOx conversion (>80%) is sustained over a wide range of feed temperatures (210–400°C). Above 200°C the selectivity of NOx reduction to N_2 increases moderately with temperature, from about 75% to nearly 100% above 450°C. Figure 14b compares the effect of the feed temperature on the NOx conversion for both cycling and steady-state operation. Shown are the conditions determined from previous experiments to give high NOx conversion (that is, rich S_N = 0.53, total cycle time = 70 s; duty cycle = 14%). A comparison to steady-state results indicates that periodic operation (rich S_N = 0.56; lean S_N = 11.7) gives NOx conversion much closer to the rich steady-state result.

Finally, we determined the effect of total cycle time on the time-averaged NOx conversion. To do this we fixed the lean feed (as before), the feed temperature (250°C), the duty cycle rich (14%), and the rich-pulse composition (S_N = 0.5), but varied the total cycle time. Figure 15 shows the results. The cycle time giving the highest conversion was about 70 s, giving a time-averaged NOx conversion over 95%. At very short cycle times, the conversion drops dramatically to a conversion of just over 40%. At very high cycle times the conversion also dropped off, although much more gradually.

Discussion

We have carried out a comprehensive performance study of the NOx storage and reduction with propylene on a model $Pt/BaO/Al_2O_3$ powder catalyst. We measured NOx storage capacity to compare and contrast short-term kinetic and longer-term factors. The effects of several key operating parameters on the time-averaged NOx conversion were determined for a single catalyst sample. Our findings help to elucidate the interaction between the storage and reduction steps and transport processes, and to reveal operating modes that give superior performance. This study builds on results of recent performance studies of the complete storage and reduction cycle (Fridell et al., 1999; Han et al., 2001; Huang et al., 2001; Lietti et al., 2001; Theis et al., 2003; Kabin et al., 2004).

The adsorptive storage of NOx on the $Pt/BaO/Al_2O_3$ powder is the critical step in the NSR process. The storage capacity was measured over a range of temperatures and NO concentrations

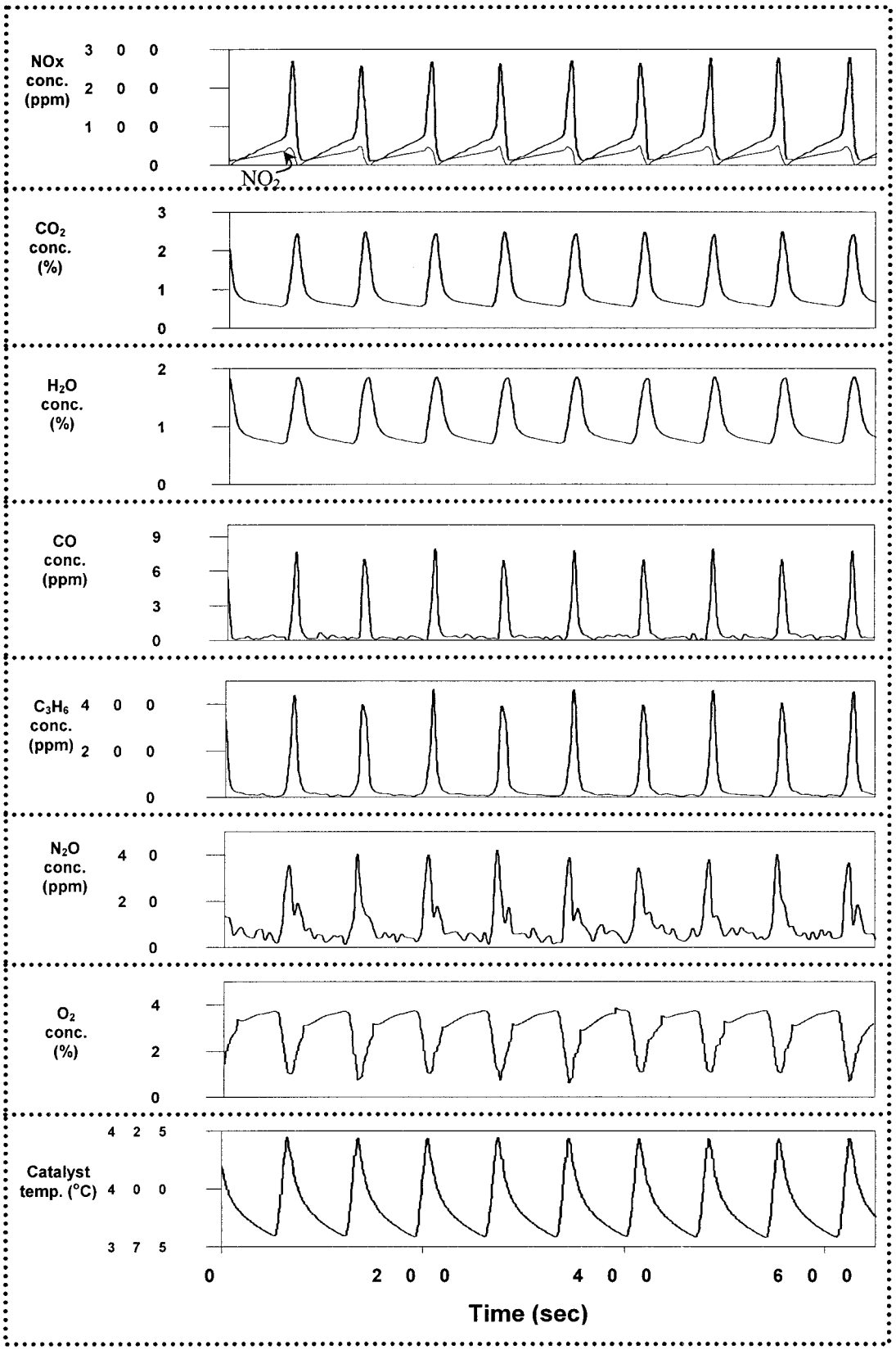

Figure 8. Concentration profiles vs. time of NOx (and NO_2), CO_2, H_2O, CO, C_3H_6, N_2O, O_2, and temperature during a typical lean/rich pulsing experiment.

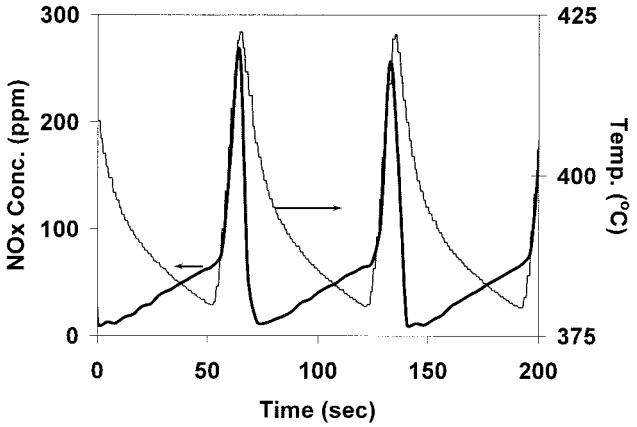

Figure 9. NOx concentration and catalyst temperature vs. time for the lean/rich pulsing experiment shown in Figure 8.

in a gas phase with excess oxygen and devoid of hydrocarbon. The transient storage occurs in two stages (Figure 3). During the first stage the entire feed of NO is trapped (that is, no NOx breakthrough). We term the amount of NOx stored in the first stage the "dynamic" storage. During the second stage the amount of NOx breakthrough slowly approaches the feed concentration of NO. Here we define the "long-time" storage as the amount of NOx stored on the catalyst when the NOx effluent concentration is equal to the NOx inlet value, within the detection limits of the FTIR (1% of the feed concentration). Although the example data shown in Figure 3 may appear to be at a saturation (or an equilibrium) storage limit, we have found that storage continues for many tens of hours, albeit very slowly. Recent TGA data we have collected indicate that true storage equilibrium between NOx and $Pt/BaO/Al_2O_3$ is achieved only after several days. The results of TGA studies currently in progress will be reported elsewhere (Muncrief et al., 2004).

The "long-time" storage data reveal a monotonic increasing dependency of the storage on gas phase NO concentration (Figure 4). In addition, the "long-time" storage is a decreasing function of temperature for a fixed NO concentration. Whereas these data are characteristic of an adsorption process, our findings suggest both kinetic and equilibrium factors associated with barium nitrate formation are operative. For one, others have reported a maximum in the storage capacity at an intermediate temperature [see, for example, the data of Mahzoul et

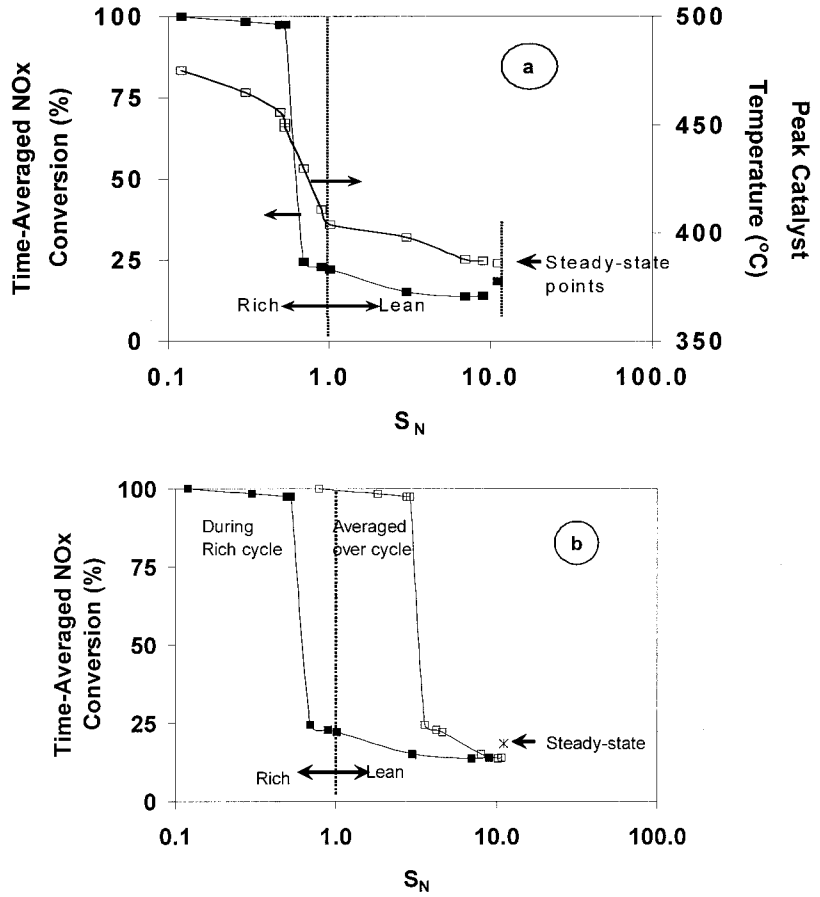

Figure 10. (a) Time-averaged NOx conversion (■) and peak catalyst temperature (□) vs. rich S_N for lean/rich cycling experiments with a continuous feed of 500 ppm NO, 5% O_2, and 1000 ppm C_3H_6. (Additional C_3H_6 is pulsed in during the rich phase with a feed temperature of 350°C). (b) Time-averaged NOx conversion for the same lean/rich pulsing experiment as in (a) vs. rich S_N (■) and time-averaged S_N (□).

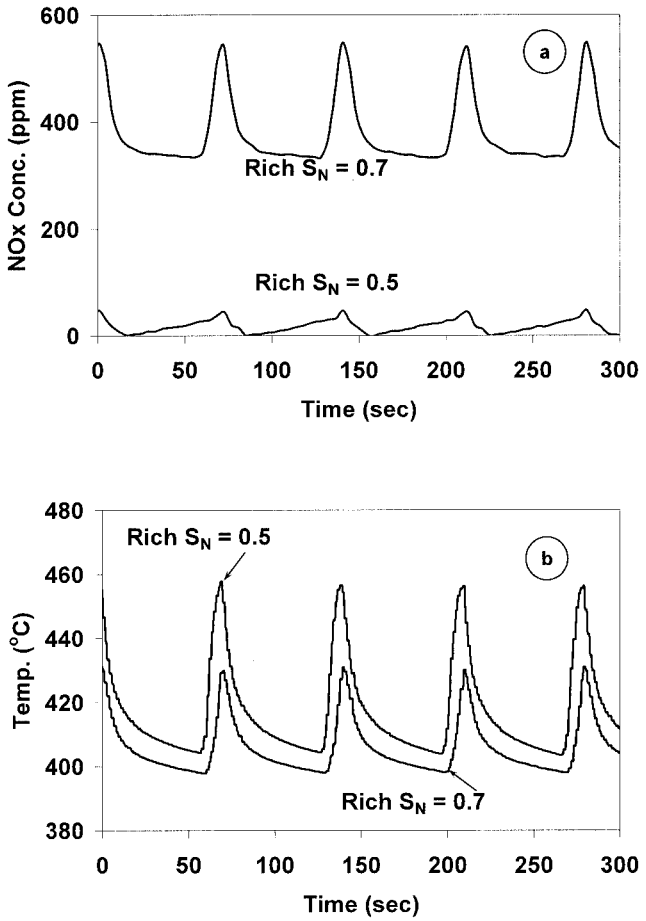

Figure 11. (a) Outlet NOx concentration vs. time for lean/rich pulsing experiments with the rich S_N = 0.7 and 0.5 with the same feed conditions as in Figure 10; (b) catalyst temperature vs. time for the pulsing experiments shown in (a).

al. (1999)]. This discrepancy may be attributable to the point noted above that it takes extended lengths of time, especially at lower temperatures, for complete NOx breakthrough to occur. At lower temperature, the rate of NOx uptake (nitrate formation) is likely kinetically limited. Olsson et al. (2001) concluded that the spillover of NO_2 from Pt crystallites to adjacent barium oxide sites is an essential step in the storage process, with an estimated activation energy of 66 kJ/mol. At higher temperature the nitrate formation is equilibrium limited, and the decreasing NOx storage with temperature promotes a less-favorable equilibrium conversion of barium carbonate to barium nitrate.

These points are underscored when examining the "dynamic" storage data, which exhibit a maximum at about 350°C (Figure 5), in close agreement with previous results (Han et al., 2001; Lietti et al., 2001). Another measure of the dynamic storage is the breakthrough time; at 350°C it is about 42 s (at the feed conditions of 200 cm^3/min, 500 ppm NO, 5% O_2). The dynamic storage capacity is about 1.5×10^{-5} mol NOx/g catalyst; this corresponds to 1 molecule of NOx stored for every 80 barium atoms. [This is only an estimate, given that we have assumed that all the NOx is adsorbed on the barium, but recognizing that some NOx adsorption may occur on the alumina support, as reported by Captain and Amiridis (1999).] In contrast, at the same conditions, 4000 s are needed for the NOx effluent concentration to approach within 1% of the inlet concentration, giving a "long-time storage" of 1.7×10^{-4} mol NOx/g catalyst, corresponding to 1 molecule of NOx for every 7 barium atoms (9%). (Following the points made above, this is not an equilibrium composition.)

The dynamic storage of the catalyst used in this study is lower than values reported in the literature. For example, Nova et al. (2002) reported a dynamic storage capacity of 1.84×10^{-4} mol NO/g catalyst (6.5 barium atoms per NO) and an "equilibrium" capacity of 5.53×10^{-4} mol NO/g catalyst (2 barium atoms per NO) at a feed temperature of 320°C and a feed gas composition of 1000 ppm NO, 3% O_2, with He balance, for a catalyst of a similar composition (that is, Pt/BaO/Al_2O_3, 1/20/100 w/w/w). These differences may be attributed to the catalyst preparation procedure. Nova et al. (2002) suggested that NOx trap catalysts prepared with alternative precursors (dinitrodiamine platinum and barium acetate) and with a different order of impregnation order (platinum before barium) gives a more active NOx trap. Specifically, a large fraction of barium atoms is postulated to be in close proximity to platinum. Fridell et al. (1999) showed that Pt is essential for NOx storage, providing adsorption sites for NO and O_2. Others have found that vicinal platinum is required for the formation of excess barium nitrate sites (Li et al., 2002). Despite the reduced capacity, the qualitative trends of the dynamic NOx uptake are in agreement with others (Fridell et al., 1997; Nova et al., 2002).

Others have observed similar multiple stages in NOx storage where there is an initial period of zero NOx breakthrough ("dynamic" storage) followed by a correspondingly long-time approach to total NOx breakthrough ("long-time" storage) (Epling et al., 2003; Tuttlies et al., 2003). This two-stage

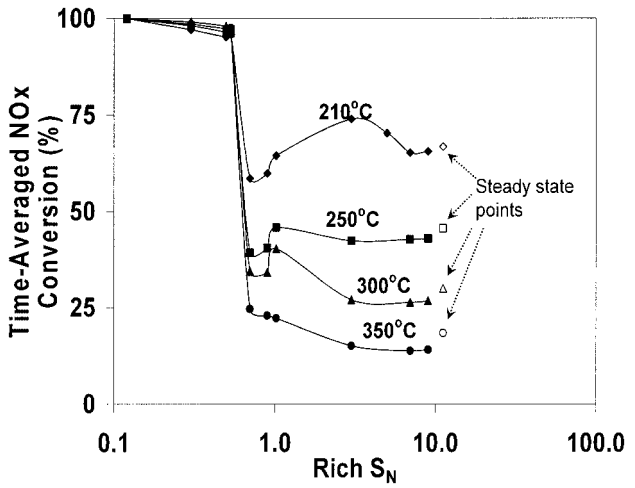

Figure 12. Time-averaged conversion vs. rich S_N for lean/rich pulsing experiments with a continuous feed of 500 ppm NO, 5% O_2, 1000 ppm C_3H_6.

Additional C_3H_6 added during the rich pulse; with a cycle time of 70 s and rich-pulse time of 10 s; at feed temperatures of 210 (◆), 250 (■), 300 (▲), 350°C (●).

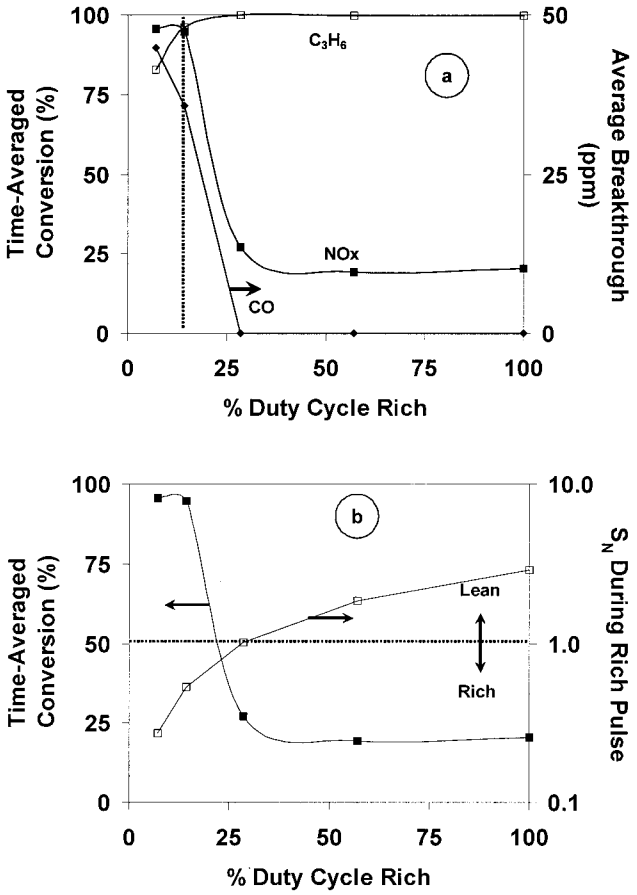

Figure 13. (a) Time-averaged NOx conversion (■), time-averaged C_3H_6 conversion (□), and time-averaged CO breakthrough (◆) vs. % duty-cycle rich for lean-rich cycling experiments with a continuous feed of 500 ppm NO, 5% O_2, a time-averaged S_N of 2.9, a cycle time of 70 s, and a feed temperature of 350°C; (b) time-averaged NOx conversion (■) and rich pulse S_N (□) vs. % duty-cycle rich for the same conditions as in (a).

storage has typically been explained by proposing multiple adsorption sites or mechanisms (Li et al., 2003; Mahzoul et al., 1999). Li et al. proposed that multiple barium sites in the form of $BaAl_2O_3$ and $BaCO_3$ are available for storage. Mahzoul et al. proposed that multiple barium sites are differentiated by their proximity to platinum. Others have shown that NOx storage occurs preferentially at barium oxide sites followed by barium carbonate sites (Nova et al., 2002). Under conditions when the catalyst surface is regenerated by reduction with hydrocarbons, the majority of the barium sites will be in the form of $BaCO_3$ (Huang et al., 2001; Nova et al., 2002). Moreover, the storage process is reported slower at barium carbonate sites. This may help to explain the existence of the complete trapping stage (I) followed by the more gradual stage (II). That is, during the first stage the NOx is trapped on the BaO sites; during the second stage the NOx is stored on the $BaCO_3$ sites. Finally, one cannot rule out the proposal of Tuttlies et al. (2003) that the prolonged second stage of NOx storage is limited by NOx diffusion through a barium nitrate shell. Further studies are needed to discriminate between the adsorptive, diffusional, and thermodynamic limitations.

The steady-state NOx reduction data over the $Pt/BaO/Al_2O_3$ catalyst are in agreement with previous findings. NOx reduction is strongly inhibited under lean conditions but nearly complete under rich conditions. For example, at a feed temperature of 250°C, the conversion decreases from nearly 100% to less than 20% as the stoichiometric number is increased from less than unity to 10 (Figure 6). However, at very low S_N the selectivity to N_2 drops to 60% (that is, 40% selectivity to N_2O). The conversion changes sharply at a stoichiometric number of unity. As seen in Figure 7a, under lean conditions the NOx conversion exhibits a sharp maximum at an intermediate temperature (210°C), which coincides with light-off of C_3H_6 (Figure 7b). On the other hand, complete NOx conversion was achieved under rich conditions for all temperatures exceeding 200°C. Under these rich conditions C_3H_6 conversion is incomplete because of total oxygen consumption. Previous findings have reported complete NOx conversion with a platinum catalyst under rich conditions (Takahashi et al., 1996) as well as the sharp maximum under lean conditions (Feeley et al., 1997). On the other hand, Han et al. (2001) reported a conversion maximum at a stoichiometric number less than unity for both Pt/Al_2O_3 and $Pt/BaO/Al_2O_3$ catalysts. They attributed these results to CO inhibition of NOx adsorption on the Pt sites. For similar stoichiometric numbers and temperatures we observed complete conversion. This may be a result of reduced site occupation by propylene, the reductant used in our study.

The effect of intermittent propylene pulsing over the $Pt/BaO/Al_2O_3$ catalyst on the transient NOx uptake and release has features observed in previous studies (Figures 8 and 9). The shape of the NOx breakthrough curve provides insight into the mechanism of the storage and reduction. (NO_2 concentration is also shown in Figure 8 to illustrate the ratio of NO to NO_2 in the product gas.) During the lean feed (500 ppm NO, 5% O_2, and 1000 ppm C_3H_6) NOx breakthrough occurs with a monotonic rise in effluent NOx concentration. Upon injection of the propylene pulse, a sharp increase in effluent NOx concentration occurs (this effect is discussed in more detail below). Finally, NOx breakthrough sharply decreases to near zero by the end of the rich pulse. This trend coincides with an increase in the effluent propylene, attributed to the nearly complete consumption of oxygen that occurs during the temporary fuel-rich conditions.

For the pulsing experiment depicted in these figures, the time-averaged feed concentration of C_3H_6 was 3570 ppm with a time-averaged NOx conversion of 97%. The time-averaged breakthrough of CO_2 is about 1%, which is in close agreement with the 3:1 CO_2:C_3H_6 oxidation stoichiometry. NOx reduction by propylene occurs during the lean phase, given that at similar conditions the steady state NOx conversion is 25%. However, the extent of reduction cannot be determined under transient conditions because of the concurrent trapping process and the lack of a measured concentration of the main reduction product, nitrogen.

As mentioned above, the injection of the propylene pulse causes an increase in effluent NOx concentration as well as a notable spike in catalyst temperature and effluent CO_2 concentration (Figure 8). The temperature increase is undoubtedly caused by the rapid Pt-catalyzed combustion of propylene,

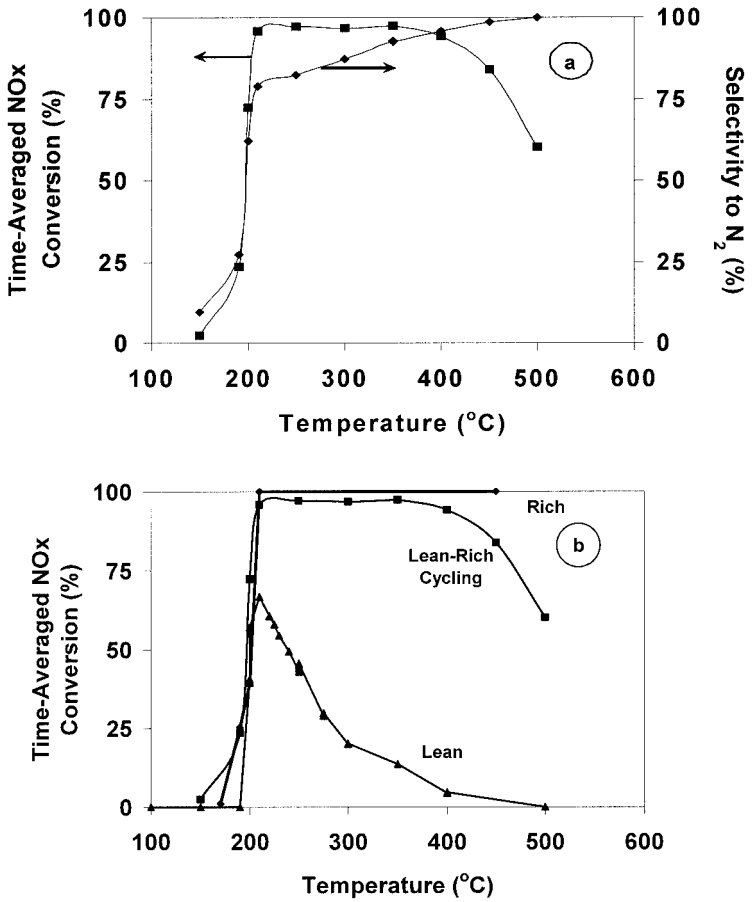

Figure 14. (a) Time-averaged NOx conversion (■) and time-averaged selectivity (◆) to N_2 vs. feed temperature for lean/rich cycling experiments with a rich pulse S_N = 0.53; with a cycle-time of 70 s, and a rich-pulse time of 10 s; (b) Steady-state rich conversion (◆) for S_N = 0.53, steady-state lean conversion (▲) for S_N = 11.2, and time-averaged NOx conversion (■) for lean/rich pulsing between S_N = 0.53 and S_N = 11.2; with 14% duty cycle rich vs. feed temperature.

made evident by the concurrent CO_2 increase (CO_2 increases to over 2.4% at its peak). The temporary increase in NOx can be attributed to two factors. First, barium nitrate decomposition commences at about 400°C (Fridell et al., 1999; Laurent et al., 2003). The oxidation exotherm is effective in driving this process. A second factor is the desorption of NOx from the Pt sites or the generation of gas phase NO by the surface reduction of barium nitrate. Previous studies of temperature-programmed desorption of NO on Pt show a NO binding energy of about 140–150 kJ/mol (Olsson et al., 2001). Theis et al. (2003) studied this "rich-purge" NOx release in great detail and found that by using shorter lean periods and adding a rhodium component to the catalyst this effect can be significantly reduced.

A high time-averaged conversion of NOx can be sustained with a pulse that is rich in propylene. The dependency of the NOx conversion on the composition of the feed gas during the propylene pulse of fixed duty cycle underscores this point (Figure 10a). The conversion is sustained above 90% if a pulse of fixed duration (duty fraction) is hydrocarbon rich, with an S_N under 0.7. The enhancement attributed to pulsing is made evident in Figure 10b, which shows the dependency of the conversion on the cycle-averaged feed composition. A net oxidizing feed with a cycle-averaged S_N as high as 3 gives an average NOx conversion of 97%. Figure 11 compares the transient NOx concentration and catalyst temperature for rich pulse S_N values of 0.7 and 0.5. A large difference in effluent NOx concentration is noted, as well as a smaller, but significant difference in catalyst temperature.

Figure 12 illustrates the feed temperature effects of the cycling in the lean and rich regimes. Nearly complete conversion of NOx (>95%) can be sustained for a rich-pulse ($S_N \leq$ 0.53) for a wide range of feed temperatures (210–350°C). When the rich-pulse S_N exceeds 0.5 the conversion drops sharply at all temperatures. The extent of the conversion drop increases as the temperature increases. These cycling data are consistent with the steady-state data presented in Figure 7. The steady-state NOx conversion in the S_N-rich regime is nearly complete for $T > 210$°C, whereas the NOx conversion in the lean regime is extremely sensitive to temperature. Figure 14a reveals how cycling can help remove the temperature restrictions that prohibit the use of this catalyst in a lean feed. As previously demonstrated in Figure 12, Figure 14a shows that with lean and rich cycling it is possible to sustain a time-averaged NOx conversion of >90% over nearly a 200°C temperature range (210–400°C).

Using these data and previous literature results, we propose

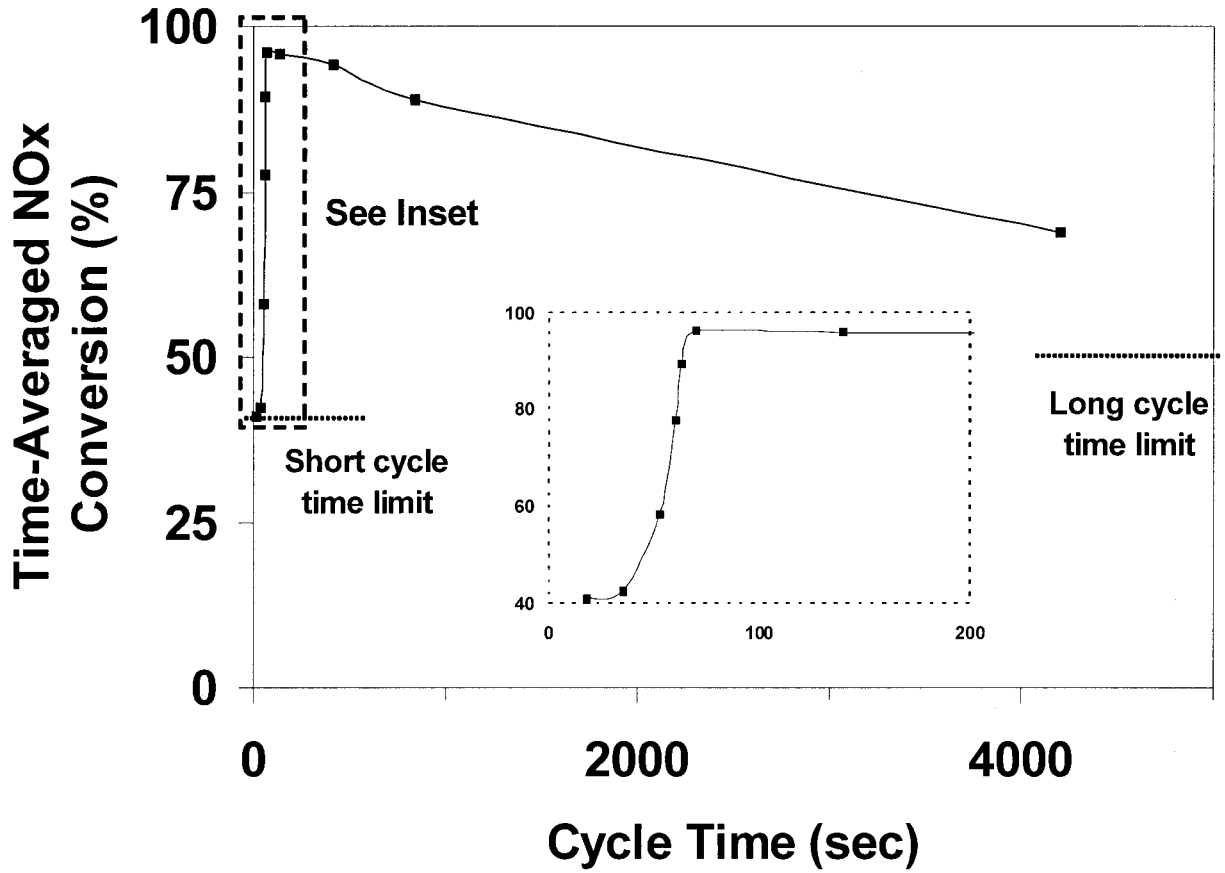

Figure 15. Time-averaged NOx conversion vs. cycle time for lean/rich pulsing experiments with 14.3% duty cycle rich, rich-pulse $S_N = 0.53$, cycle-averaged $S_N = 2.9$, and a feed temperature of 350°C.

the phenomenological mechanism depicted in Figure 16 for the storage and reduction of NOx with propylene on a Pt/BaO/Al_2O_3 catalyst. The mechanism is intended to convey the overall reactions occurring during a typical lean (storage)–rich (reduction) cycle. The mechanism presumes that the main form of barium in the presence of hydrocarbon is $BaCO_3$. Barium carbonate sites have also been observed by examining the reduced surface with infrared spectroscopy (IR) analysis (Rodrigues et al., 2001). We have observed, as have others, that

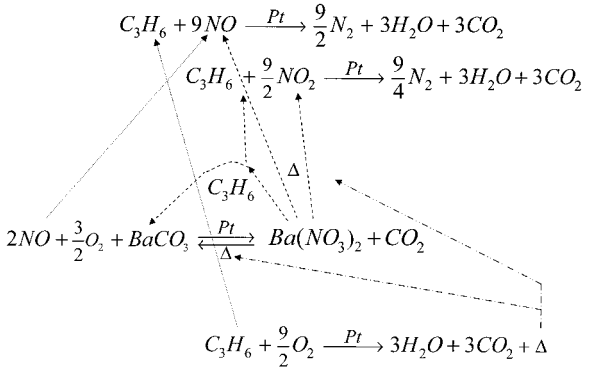

Figure 16. Proposed phenomenological mechanism for lean/rich NOx storage and reduction on Pt/BaO/Al_2O_3 catalyst.

CO_2 desorbs when NOx is introduced to the reduced catalyst. The formation of barium nitrate occurs by the sequential steps of NO and O_2 adsorption and reaction on Pt, followed by nitration of the $BaCO_3$, evolving CO_2. The addition of propylene in the presence of O_2 leads to catalytic oxidation on the Pt. The combustion generates heat and deep oxidation products. $Ba(NO_3)_2$ decomposes at sufficiently high temperature (Mahzoul et al., 1999), forming BaO, which quickly converts to the carbonate (in the presence of hydrocarbon and CO_2), and a mixture of NO and NO_2. As mentioned above, $Ba(NO_3)_2$ may also be reduced by adsorbed propylene (fragments) during the period of oxygen depletion. These two overall steps complete the barium cycle and also help to explain the burst of NOx (especially at higher temperatures) at the point of propylene injection. Finally, adsorbed NOx then reacts with propylene by standard selective reduction on Pt. This occurs with high conversion when oxygen is depleted during the periodic rich conditions.

A propylene concentration in moderate excess of stoichiometric requirements ($S_N \cong 0.5$–0.7) for complete oxidation is needed to achieve a high conversion of NOx. During the temporary rich conditions of the pulse, previously oxygen covered Pt sites become vacant, enabling the adsorption and reaction of NO and propylene. Whereas the shift from low to high conversion occurs at $S_N = 1$ under steady-state conditions, the shift occurs at $S_N \cong 0.6$ under cycling conditions. This may

be explained by an accumulation of oxygen on the surface during the lean period of cycling. Olsson et al. (2002) modeled NOx storage and reduction by propene (without excess O_2) on $Pt/BaO/Al_2O_3$. They predicted that during the lean phase most platinum sites become covered by oxygen; during the rich phase the hydrocarbon must first react with the surface oxygen atoms to form CO_2 and H_2O before it may adsorb and dissociate on the surface of the platinum and react with the adsorbed NOx. Another factor may be a reduction in the propylene concentration during the pulse resulting from dispersion.

Figure 13 underscores the importance of the rich pulse during cycling. When a fixed amount of reductant propylene (in this case 0.67 cm^3) is injected over a period of 10 s the time-averaged NOx conversion is >90%. However, the same amount of propylene injected over a period of 20 s results in a conversion of <30%. A high conversion is sustained only if the pulse is sufficiently rich ($S_N < 0.8$). Thus, pulsing should create a temporary rich, oxygen-depleted condition, freeing up Pt sites for selective reduction to occur. Moreover, the elevated temperature, caused by the oxidation, accelerates the reduction during the temporary rich conditions.

Figure 15 shows that rich and lean cycling is robust over a wide range of cycle times. The time-averaged NOx conversion exceeds 90% for cycle times spanning 70–420 s. In this series of experiments the propylene duty cycle was fixed at 14.3%, giving a cycle-averaged stoichiometric number of 2.9. The NOx conversion achieves a maximum at an intermediate cycle time (70 s). The conversion drops to 40% at short cycle times (<35 s) and to 60% at long cycle times (>4200 s). At very short and very long cycle times with fixed rich duty fraction, the beneficial effects of periodic operation diminish. The conversion decrease to the left of the maximum is a consequence of two factors. The first factor is the mixing of rich and lean feeds that occurs upstream of the reactor. We carried out independent measurements of propylene pulsing to a blank reactor. These tests confirmed that the intended amount of propylene fed was delivered but that dispersion caused a dilution of the propylene. The dilution effect was larger at shorter cycle times, indicating an effect of the feed system. This would cause the time-averaged conversion maximum to occur at a somewhat higher cycle time. The second factor is that the storage catalyst is unable to respond quickly enough to the rapid pulsing. Both factors will cause the time-averaged conversion to approach a pseudo steady-state value corresponding to a mixed feed (in this case $S_N = 2.9$). Indeed, the results show that the conversion (41%) is close to the measured steady-state conversion of 45% for feed with $S_N = 2.9$. At long cycle times the trap has ample time to respond, and the trap approaches steady state during the lean and rich phases. The time-averaged conversion (X_{NOx}) is approximated by a weighted average of the steady-state conversions; that is,

$$X_{NOx} = wX_r^{ss} + (1 - w)X_l^{ss} \quad (2)$$

where w is the rich fractional duty cycle, X_r^{ss} is the steady-state conversion at the rich feed composition, and X_l^{ss} is the corresponding conversion at the lean feed composition. Applying $w = 0.14$, $X_r^{ss} = 100\%$, and $X_l^{ss} = 45\%$ gives $X = 53\%$. The data reveal that cycle times exceeding 5000 s are needed for the trap to approach this asymptotic value.

Conclusions

Steady-state selective catalytic reduction of NOx is ineffective under lean conditions. We have carried out NOx storage and reduction on a $Pt/BaO/Al_2O_3$ powder catalyst using propylene as the reductant.

The study indicates that the periodic addition of propylene to the catalyst bed can result in time-averaged NOx conversions approaching the rich NOx conversion limit obtained under steady-state conditions. In addition, the propylene injection policy has an important effect on NOx conversion, in terms of feed composition, reductant pulse duration, overall cycle time, and temperature. To achieve a high time-averaged NOx conversion, the gas composition during the propylene injection must be net reducing ($S_N < 1$). Most effective are short pulses with high propylene concentration. Least effective is the dilution of a fixed amount of propylene over the entire cycle. Cycle time is also an important factor, with the time-averaged NOx conversion achieving a maximum value at an intermediate cycle time. Cycle times of very short or very long duration do not exploit the benefits of lean/rich cycling. For shorter cycle times the time-averaged conversion approaches a steady-state conversion as if the lean and rich streams had been premixed; for much longer cycle times the time-averaged conversion is a weighted average (by duty fraction) of the steady-state conversions obtained with the lean and rich feeds. The high conversions were sustained over a wide temperature window (200–400°C). Below 200°C the propylene oxidation extinguishes; above 400°C the conversion decreases as a consequence of reversible nitrate decomposition and NO desorption. A simple storage–reduction cycle is proposed that elucidates the main findings in the study. The key factor for high NOx conversion is the temporal production of oxygen-deficient conditions coupled with high catalyst temperatures, both resulting from the intermittent catalytic oxidation of propylene.

Ongoing studies carried out in our lab include experimenting with NSR on monolith catalysts with a $Pt/BaO/Al_2O_3$ washcoat, elucidating the proposed mechanism by incorporating modeling of the system, the use of other reductants such as high molecular weight hydrocarbons (to simulate diesel fuel) and H_2/CO (to simulate partially oxidized diesel fuel), and experiments under *in situ* FTIR to elucidate the surface species formed during storage and reduction.

Acknowledgments

The support of the State of Texas Advanced Technology Program (ATP) is gratefully acknowledged. We also acknowledge fruitful technical discussion with Dr. Yuejin Li of Engelhard Corp.

Literature Cited

Amberntsson, A., M. Skoglundh, S. Ljungstrom, and E. Fridell, "Sulfur Deactivation of NOx Storage Catalysts: Influence of Exposure Conditions and Noble Metal," *J. Catal.*, **217**, 253 (2003).

Armor, J. N., and K. Li, "The Effect of SO_2 on the Catalytic Performance of Co-ZSM-5 and Co-Ferrierite for the Selective Reduction of NO by CH_4 in the Presence of O_2," *Appl. Catal. B Environ.*, **5**, 257 (1995).

Bogner, W., M. Kramer, B. Krutzsch, S. Pischinger, D. Voigtlander, G. Wenninger, F. Wirbeleit, M. S. Brogan, R. J. Brisley, and D. E. Webster, "Removal of Nitrogen Oxides from the Exhaust of a Lean-Tune Gasoline Engine," *Appl. Catal. B Environ.*, **7**, 153 (1995).

Borup, R., M. Inbody, T. Semelsberger, J. Tafoya, and W. Parkinson, "Fuel Effects on Fuel Reforming Operation and Start-up for Transportation

Fuel Cell Systems," Paper No. 99f, AIChE Spring Meeting, New Orleans, LA (2003).
Burch, R., and P. J. Millington, "Selective Reduction of Nitrogen Oxides by Hydrocarbons under Lean-Burn Conditions Using Supported Platinum Group Metal Catalysts," *Catal. Today*, **26**, 185 (1995).
Captain, D. K., and M. D. Amiridis, "In Situ FTIR Studies of the Selective Catalytic Reduction of NO by C_3H_6 over Pt/Al_2O_3," *J. Catal.*, **184**, 377 (1999).
Clerc, J. C., "Catalytic Diesel Exhaust Aftertreatment," *Appl. Catal. B Environ.*, **10**, 99 (1996).
Czamecki, L., J. Fuhr, R. Oegema, and R. Hilton, "SCONOx™-Ammonia Free NOx Removal Technology for Gas Turbines," *Proc. of the 2000 International Joint Power Generation Conference,* Miami Beach, FL (2000).
Diesel Technology Forum, Demand for Diesels: The European Experience, http://www.dieselforum.org/whitepaper/downloads/europeanexperience.pdf (2001).
Epling, W. S., G. C. Campbell, and J. E. Parks, "The Effects of CO_2 and H_2O on the NOx Destruction Performance of a Model NOx Storage/Reduction Catalyst," *Catal. Lett.*, **90**, 45 (2003).
Farrauto, R. J., and K. E. Voss, "Monolithic Diesel Oxidation Catalysts," *Appl. Catal. B Environ.*, **10**, 29 (1996).
Feeley, J., M. Deeba, and R. J. Farrauto, "A Catalytic NOx Management System for Lean Burn Engines," *Catalysis and Automotive Pollution Control IV: Proc. of the Fourth International Symposium,* Brussels, Belgium, N. Kruse, A. Frennet, and J.-M. Bastin, eds., Elsevier, Amsterdam, Vol. 116, pp. 529–536 (1997).
Fridell, E., M. Skoglundh, S. Johansson, B. Westerberg, A. Torncrona, and G. Smedler, "Investigations of NOx Storage Catalysts," *Catalysis and Automotive Pollution Control IV: Proc. of the Fourth International Symposium,* Brussels, Belgium, N. Kruse, A. Frennet, and J.-M. Bastin, eds., Elsevier, Amsterdam, Vol. 116, pp. 537–547 (1997).
Fridell, E., M. Skoglundh, B. Westerberg, S. Johansson, and G. Smedler, "NOx Storage in Barium-Containing Catalysts," *J. Catal.*, **183**, 196 (1999).
Frost, J. C., and G. Smedler, "Control of NOx Emissions in Diesel Powered Light Vehicles," *Catal. Today*, **26**, 207 (1995).
Han, P.-H., Y.-K. Lee, S.-M. Han, and H.-K. Rhee, "NOx Storage and Reduction Catalysts for Automotive Lean-Burn Engines: Effect of Parameters and Storage Materials in NOx Conversion," *Top. Catal.*, **16/17**, 165 (2001).
Herzog, P. L., "Diesel Engine Development Routes Towards Very Low Emissions," *Catalysis and Automotive Pollution Control IV: Proc. of the Fourth International Symposium,* Brussels, Belgium, N. Kruse, A. Frennet, and J.-M. Bastin, eds., Elsevier, Amsterdam, Vol. 116, pp. 35–48 (1997).
Huang, H. Y., R. Q. Long, and R. T. Yang, "The Promoting Role of Noble Metals on NOx Storage Catalyst and Mechanistic Study of NOx Storage under Lean-Burn Conditions," *Energy Fuels*, **15**, 205 (2001).
Kabin, K., R. Muncrief, and M. P. Harold, "NOx Storage and Reduction on a Pt/Bao/Alumina Monolithic Storage Catalyst," *Catalysis Today,* in press (2004).
Ladommatos, N., S. Abdelhalim, and H. Zhao, "The Effects of Exhaust Gas Recirculation on Diesel Combustion and Emissions," *Int. J. Eng. Res.*, **1**, 107 (2000).
Laurent, F., C. J. Pope, H. Mahzoul, L. Delfosse, and P. Gilot, "Modeling of NOx Adsorption over NOx Adsorbers," *Chem. Eng. Sci.*, **58**, 1793 (2003).
Lee, H.-T., and H.-K. Rhee, "Steam Tolerance of FE/ZSM-5 Catalyst for the Selective Catalytic Reduction of NOx," *Korean J. Chem. Eng.*, **19**, 574 (2002).
Li, X., M. Meng, P. Lin, Y. Fu, T. Hu, Y. Xie, and J. Zhang, "Study of the Relationship between Microstructure and Performance for NOx Storage Catalysts," *Trans. Inst. Chem. Eng.*, **80**, 190 (2002).
Li, X., M. Meng, P. Lin, Y. Fu, T. Hu, Y. Xie, and J. Zhang, "A Study on the Properties and Mechanisms for NOx Storage over $Pt/BaAl_2O_4$–Al_2O_3 catalyst," *Top. Catal.*, **22**, 111 (2003).
Lietti, L., P. Forzatti, I. Nova, and E. Tronconi, "NOx Storage Reduction over Pt–Ba/γ-Al_2O_3 Catalyst," *J. Catal.*, **204**, 175 (2001).
Lox, E. S., B. H. Engler, and E. Koberstein, "Diesel Emission Control," *Catalysis and Automotive Pollution Control II: Proc. of the Second International Symposium,* A. Crucq, ed., Brussels, Belgium, Elsevier, Amsterdam, Vol. 71, pp. 291–321 (1990).
Mahzoul, H., J. F. Brilhac, and P. Gilot, "Experimental and Mechanistic Study of NOx Adsorption over NOx Trap Catalysts," *Appl. Catal. B Environ.*, **20**, 47 (1999).
Manufacturers of Emission Controls Association (MECA), *The Impact of Sulfur in Diesel Fuel on Catalyst Emission Control Technology*, MECA, Washington, DC (1999).
Matsumoto, S. I., "Catalytic Reduction of Nitrogen Oxides in Automotive Exhaust Containing Excess Oxygen by NOx Storage–Reduction Catalyst," *Cattech*, **4**, 102 (2000).
Miyoshi, T., S. I. Matsumoto, K. Katoh, T. Tanaka, J. Harada, N. Takahashi, K. Yokota, M. Sugiura, and K. Kasahara, "Development of New Concept Three-Way Catalyst for Automotive Lean-Burn Engines," *SAE J. Automot. Eng.*, **950809**, 1361 (1995).
Muncrief, R., P. Khanna, K. Kabin, and M. P. Harold, "Mechanistic and Kinetic Studies of NOx Storage and Reduction on $Pt/BaO/Al_2O_3$," *Catalysis Today,* in press (2004).
Narula, C. K., S. R. Nakouzi, R. Wu, C. T. J. Goralski, and L. F. J. Allard, "Evaluation of Sol–Gel Processed BaO–Al_2O_3 Materials as NOx Traps," *AIChE J.*, **47**, 744 (2001).
Nova, I., L. Castoldi, L. Lietti, E. Tronconi, and P. Forzatti, "On the Dynamic Behavior of 'NOx-Storage/Reduction' $Pt-Ba/Al_2O_3$ Catalyst," *Catal. Today*, **75**, 431 (2002).
Olsson, L., E. Fridell, M. Skoglundh, and B. Andersson, "Mean Field Modelling of NOx Storage on $Pt/Ba/Al_2O_3$," *Catal. Today*, **73**, 263 (2002).
Olsson, L., H. Persson, E. Fridell, M. Skoglundh, and B. Andersson, "A Kinetic Study of NO Oxidation and NOx Storage on Pt/Al_2O_3 and $Pt/BaO/Al_2O_3$," *J. Phys. Chem. B*, **105**, 6895 (2001).
Ott, K. C., N. C. Clark, and J. A. Rau, "Hysteresis in Activity of Microporous Lean NOx Catalysts in the Presence of Water Vapor," *Catal. Today*, **73**, 223 (2002).
Rodrigues, F., L. Juste, C. Potvin, J. F. Tempere, G. Blanchard, and G. Djega-Mariadassou, "NOx Storage on Barium-Containing Three-Way Catalyst in the Presence of CO_2," *Catal. Lett.*, **72**, 59 (2001).
Salasc, S., M. Skoglundh, and E. Fridell, "A Comparison between Pt and Pd in NOx Storage Catalysts," *Appl. Catal. B Environ.*, **36**, 145 (2002).
Shelef, M., "Selective Catalytic Reduction of NOx with N-Free Reductants," *Chem. Rev.*, **95**, 209 (1995).
Takahashi, N., H. Shinjoh, T. Iijima, T. Suzuki, K. Yamazaki, K. Yokota, H. Suzuki, N. Miyoshi, S. I. Matsumoto, T. Tanizawa, T. Tanaka, S.-S. Tateishi, and K. Kasahara, "The New Concept 3-Way Catalyst for Automotive Lean-Burn Engine: NOx Storage and Reduction Catalyst," *Catal. Today*, **27**, 63 (1996).
Texas Commission of Environmental Quality (TCEQ), State Implementation Plan (SIP): Complying with the Clean Air Act in Texas. http://www.tnrcc.state.tx.us/oprd/sips/ (2003).
Theis, J. R., J. A. Ura, J. J. Li, G. G. Surnilla, J. M. Roth, and C. T. J. Goralski, "NOx Release Characteristics of Lean NOx Traps during Rich Purges," *SAE Int.*, **2003-01-1159**, 5 (2003).
Traa, Y., B. Burger, and J. Weitkamp, "Zeolite-Based Materials for the Selective Catalytic Reduction of NOx with Hydrocarbons," *Micropor. Mesopor. Mater.*, **30**, 3 (1999).
Tuttlies, U., V. Schmeisser, and G. Eigenberger, "A New Simulation Model for NOx Storage Catalyst Dynamics," Proc. of the Sixth International Congress on Catalysis and Automotive Pollution Control, Brussels, Belgium (2003).
van Kooten, W. E. J., H. P. A. Calis, and C. M. van den Bleek, "Stability of Cerium Exchanged Zeolite Catalysts for the Selective Catalytic Reduction of NOx in Simulated Diesel Exhaust Gas," Catalysis and Automotive Pollution Control IV: Proc. of the Fourth International Symposium, Brussels, Belgium, N. Kruse, A. Frennet, and J.-M. Bastin, eds., Elsevier, Amsterdam, Vol. 116, pp. 357–366 (1997).

Manuscript received Sep. 30, 2003, and revision received Jan. 27, 2004.